Chemometric approach to evaluate the chemical behavior of rainwater at high altitude in Shaune Garang catchment, Western Himalaya

Ramesh Kumar (rameshkumar9234@gmail.com)
Central University of Rajasthan
Rajesh Kumar
Central University of Rajasthan
Atar Singh
Central University of Rajasthan
Mohammad Arif
Forest & Climate Change (MoEFCC), Govt. of India
Pankaj Kumar
Forest & Climate Change (MoEFCC), Govt. of India
Anupma Kumari
Patna University

Research Article

Keywords:

Posted Date: June 17th, 2022

DOI: https://doi.org/10.21203/rs.3.rs-1305725/v1

Abstract

The present research study was performed to analyze the chemical behavior of rainwater in the Shaune Garang catchment (32.19°N, 78.20°E) in the Baspa basin, which is located at a high elevation (4221m above mean sea level). The volume-weighted mean (VWM) pH value of rainwater ranged between 4.59 and 6.73, with an average of 5.47 0.69, indicating that alkaline rainfall events primarily influenced the catchment during the study. The total ionic strength in the rainwater ranged from 113.4 to 263.3 μeq/l with an average of 169.1 ± 40.4 μeq/l. The major dominant cations were measured as Ca^{2+} (43.1%) and Na^{+} (32%) and anions, Cl^{-} (37.7%), SO_4^{2-} (28.7%) and NO_3^{-} (23.8%) in rainwater. The fraction of NO_3^{-} + Cl^{-} with SO_4^{2-} was measured as 2.3, which specifies sour faces of rainwater due to HNO_3^{-}, H_2SO_4, and HCl. Chemometric evaluation of rainwater within the Shaune Garang catchment, including Principal Component and Factor analysis. According to the findings, the composition of rainwater in the pristine Himalayas is moreover influenced by man-made and natural causes of pollutants due to long-distance transference. The air mass trail investigation demonstrates the impact of airborne primary and secondary particle transportation that influences the chemical composition of precipitation.

Introduction

The Himalayan region provides a unique ecosystem and resources, sources of many rivers in nearby countries like India, Pakistan, China. Glaciers in the high-altitude area serve as "water towers" and provide significant amounts of meltwater to the downstream population [1]. However, the retreat of the Himalayan glaciers due to alteration and variation in the precipitation pattern in the regime impacts climate change [2]. Also, atmospheric pollution such as aerosol, dust, particulate matter threatens the Himalayan region. In recent years, atmospheric pollutants have increased to an extreme degree due to the lucrative growth in population, economics, and energy use [3-4]. According to a modern assessment report [5], air contamination is the sixth prominent threat for death globally, killing more people than food scarcity, alcohol consumption, and physical laziness combined. Additionally, more people die because of air contamination-related diseases than automobile accidents. Rainwater chemistry studies reflect the air emissions quality provided to the atmosphere by either natural or unnatural sources [6]. It aids in determining the comparative significance of various causes and forecasting likely acidification buffering ability in the future [7]. According to some studies, rainwater acidity has become a significant environmental hazard, affecting soil texture, groundwater quality, vegetation, and plants, as well as human healthiness [8-9]. As a result, World Meteorological Organization established the Global Atmospheric Watch program to monitor changing rainwater chemistry through a network of stations worldwide [10]. Additionally, the chemical configuration of rainwater is directly related to different factors such as native radiations, contaminant transportation, climatic situations, and the size of the drop. Atmospheric particles play a critical role in forming clouds and rain and influence the distribution of energy in the atmosphere. The particles emitted by the natural and anthropogenic sources get conveyed to elongated distances from the origin and sifted by different atmospheric mechanisms [11-12]. The presence of particles in the atmosphere is determined by a variety of mechanisms, including the washout

process known as below-cloud scavenging and in-cloud scavenging known as rainout. The washout process removes coarse mode particles from the atmosphere, whereas the rainout practice integrates fine-mode particles [13-14]. The climatic impact of the atmospheric particles is not well understood due to the lack of documented study regarding rainwater's physical and chemical composition [15]. The study on rainwater chemistry has been done to determine the physio-chemical composition and its possible sources over several parts of the world, including India [16-19, 12], but such studies are rare over the Himalayan region. Hence, rainwater chemistry is essential to understand the mechanism of pH and EC fluctuation at greater altitudes in the Himalayan region. Significant research has been conducted in the Himalayan region for determining the chemistry of rainwater [20-23]. Therefore, the primary goal of the present investigation is to define the chemical properties of rainwater and assess the impact of anthropogenic and natural emissions sources in rainwater. Furthermore, statistical techniques and trajectory analysis are performed to classify potential causes of rainwater composition. Besides these, probably no documented works are available on rainwater chemistry in the high altitude in Sangla Valley Baspa basin. Therefore, we have focused on a detailed study to fill the research gap covering physical and chemical characteristics and possible nutrient sources. In addition, this study could be significant for a better understanding of the role of the weathering process and hydrological process in the catchment. A special focus will be directed to the multivariate statistical assessment of rainwater chemistry.

Result And Discussion

Data screening and quality control

The sampling protocol was considered with the proper care in collecting and preserving the rainwater samples until the complete chemical analysis. In addition, the rainwater samples were excluded that were found any traces, filthy, messy, or contaminated with dust at the sampling site. The data acquired through the chemical analysis were tested through the ion balance method. Data were examined to ensure analytical quality, considering calibration and blank dimensions. The principle of electro-neutrality depicts the eminence of chemical analysis, which can be measured to some extent by the ionic balance in particular occurrences in the samples. The cation/anion ratio in rainwater samples was observed 0.74 and 1.56, with a mean value of 1.10±0.24. There was a significant linear regression (r = 0.60) between the sum of anions and cations **(Figure 1).** The outcome designates that the quality of data is high and precise enough for further chemical analysis. In the current analysis, the deviation of ≤ 40.4 for the total ion concentration of 169.14 µeq/l is within the acceptable range of 113.45 – 263.33 µeq/l. However, the sample location is located at a high altitude, and such ion-balance deviations may be caused by fluctuations in lower and higher ion concentrations and the presence of weak organic acids. A prevalent organic acid in the atmosphere, coupled with the H^+ ion, is likely to evaporate fast in non-preserved water samples and their quantities were lower in rainwater samples [18]. The volume-weighted mean (VWM) concentrations of the observed chemical species in the Shaune Garang catchment rainwater were calculated as follows [24]:

$$\text{VWM}\left(\frac{\mu\text{eq}}{\text{l}}\right) = \frac{\sum_{i=0}^{n} Ci\ Pi}{\sum_{i=0}^{n} Pi} \qquad \textit{Equation 1}$$

Ci denotes the concentration of a specific chemical species (μeq/l), while Pi and N denote the quantity of rainfall for each event (in mm) and the total number of rainfall events, respectively.

pH and EC variability in rainwater

The pH value of rainwater indicates the presence of major ionic constituents, either from atmospheric gas assimilation or anthropogenic sources. Significant ionic species in rainwater are caused by in-cloud and sub-cloud scavenging processes in the atmosphere [25]. Even though sulfuric and nitric acid is formed from nitrogen and Sulphur oxides, they freely dissolve in cloud water and produce extra hydrogen ions. Furthermore, higher levels of carbon dioxide (CO_2) in the atmosphere dissolve in cloud water and produce weak carbonic acid [23]. pH (< 5.6) (i.e., atmospheric CO_2 balance) indicates the presence of acidic species in the ionic composition of rainwater. In contrast, a pH value of more than 5.6 specifies the existence of basic species, particularly crustal species, or mineral dust [26]. The pH of rainwater fluctuated from 4.59 to 6.73 and the mean value with the standard deviation of 5.47 ± 0.69 during the sampling period, indicating a mixture of anthropogenic and natural chemical constituents in the catchment (**figure S1a**). The lowest pH value observed was 4.59 on 3 September 2017, having 7.28 mm rainfall, showing episodic high acidity of rainwater in the catchment. The high pH value was measured on 13 September 2017, when 36.25 mm rainfall was noted with the high alkaline aerosols (Ca^{2+}) presence. Several studies at high altitudes in India and around the world report the average pH value of rainwater 5.10- 6.40. The variation in the pH and EC values of rain events during the study period over the sampling site is presented in **figure S1b**. In the Himalayas, at Kullu, the pH value of rainwater was reported ranging from 5.16 – 3.36 [21], while at Darjeeling, it varied from 5.0 ± 0.8 [22]. The VWM pH of the rainwater was observed as 5.56 ± 0.29, indicating the mixture of anthropogenic and natural chemical constituents in the rainwater of Shaune Garang catchment. In addition, the other fundamental constituent of rainwater is the specific conductivity, which was considered to check the quality of rainwater in the Shaune Garang catchment. The average specific conductivity observed in this valley was 13 to 36 μS/cm, with an average value of 22.31 ± 7.3. The specific conductivity in this catchment is lower than the reported value of 7 to 57 μS/cm in the Himalayan region [27 28]. To understand the correlation between specific conductivity and the sum of cations and anions in the Western Himalayan region, specific conductivity was plotted against the sum of cations and anions. The findings show a stronger correlation with anions (R^2 = 0.89) than with cations (R^2 = 0.60), as presented in figure 2.

For determining the rain acidity, linear regression analysis between the ionic concentration of hydrogen ion (H^+) in rainwater and rainfall amount is schemed (**Figure S2**). In general, the analysis results suggested that the concentration of H^+ increases with rainfall. The lowest pH value of 4.59 corresponds

to a high hydrogen ion concentration (H^+= 3.62 µeq/l) with 1.3 mm of rainfall. Furthermore, the highest pH of 6.73 (H^+= 1.48 µeq/l) correlates with a little concentration of hydrogen ions (H^+= 0.4) in 0.04 mm of rainfall in the Shaune Garang catchment (**Figure 3**). The significant rain in the middle of the sampling period was a major factor in the dilution of hydrogen ions. Seasonal variations in rainfall amount and air quality have an impact on these.

Chemical constituents of rainwater

A rigorous statistical analysis was done to determine the mean, volume-weighted mean (VWM), minimum, maximum, standard deviation, and standard error for each major ion and pH provided in Table 1. The charge balance error (CBE) analysis of the chemical composition of dissolved ions in rainwater demonstrated the dataset's accuracy. As a result, the following empirical formula was used to calculate it:

$$CBE = \frac{(TZ^+ - TZ^-)}{(TZ^+ + TZ^-)} \times 100$$

Where, TZ^+ = Total cation

TZ^- = Total anion *Equation 2*

During the melting period, the error in charge balance between total cation (TZ +) and total anion (TZ -) was found to be (6%), indicating that the dataset is more accurate. Table S1 summarizes the chemical composition of rainwater samples collected from the Shaune Garang glacier during the 2017 study period. The rainwater ionic composition's volume-weighted mean (VWM) was 167.54 µeq/l, indicating low atmospheric pollution concentrations in the Shaune Garang catchment. Mean cation values were 86.13 µeq/l, and anions were 83.01 µeq/l. The outcome demonstrates the supremacy of cations over anions in the catchment. The mean values of ionic species concentrations (169.14 µeq/l) are higher than the median values (157.32 µeq/l), indicating an irregular dispersal of ionic species with skewness to the left. The median and average concentrations show an analogous configuration. Therefore, VWM is used to recognize the greater concentrations during brief periods of rain and to evade clean rain diluting and influencing the rainwater concentration [29]. Among all ionic components, calcium contributed maximum (22.35 %), followed by chloride (17.72 %), sodium (16.39 %), sulphate (13.62 %), nitrate (11.81 %), magnesium (8.97 %), bicarbonate (5.06 %) and potassium (4.08 %). Although, the acidic nature of water generally initiates due to the influence of sulfuric and nitric acid and the neutralization process by cations such as $Ca^{2+}$and Mg^{2+} [30]. The input of cations and anions in rainwater during the study period was 48.22 and 51.78 %, correspondingly. The outcome shows that the higher contributions of anions are due to transference from distant sources instead of localized sources [22]. Calcium (Ca^{2+}) was observed as the dominant ionic species with a much lower influence of SO_4^{2-} and NO_3^- (13.62 and 11.81 %).

Similarly, the sea salts such as Na^+ are contributing 16.39 %, and Cl^- contributing 17.72 % indicated the transportation from distant sources and influenced by the sea. Notably, SO_4^{2-} was the second greatest abundant species, and K^+ was the least abundant species among the anions during the study period. Figure S4 shows the percentage contribution of measured ionic species in the rainwater of Shaune Garang catchment. The result shows that the maximum contribution in the ionic concentration in the rainwater is of Ca^{2+} (22.35 %) and minimum from K^+ (4.08 %). This might be due to considerable contribution from marine sources in NaCl sea salt [9] and the crustal source in the form of $Ca^{2+}$and Mg^{2+}. In addition, the contribution from anthropogenic sources SO_4^{2-} (13.62 %), NO_3^- (11.81 %), and K^+ (4.08 %) is also observed in rainwater composition, which might be due to the resident wood-burning activities [31]. Though, a significant alternative source of the perceived ionic composition in the rainwater might be dust and sea salt transported from other areas. However, the highest VWA ionic species concentration in the rainwater was Ca^{2+}, $Cl^{+,}$ Na^+, $SO4^{2-}$, and Mg^{2+}. Volume weighted mean pH was detected 4.59 and reached as high as 6.73 with an increase in Ca^{2+} (56.23 µeq/l) in rainwater in the catchment. This suggests that Ca^{2+} be the primary neutralizing agent in rainwater. Though, Mg^{2+} and K^+ can defuse acidity produced due to SO_4^{2-} and NO_3^- to regulate the pH of rainwater in the alkaline range.

Ionic ratio of rainwater

Rainwater quality measures a characteristic function such as acidic and alkaline ingredients. The present research found that the ionic strength and concentration in the rainwater during the study period was calculated as 169.14 µeq/l. Although, the acidic nature of water generally initiates due to the influence of nitric and sulfuric acid and the neutralization process by cations containing Ca^{2+}+ Mg^{2+} [21]. Apart from this, the ionic ratio has been calculated to apprehend the comparative involvement of Sulphuric and nitric acid rain formation in the study area.

In addition, fractional acidity (FA) was calculated to understand the acid neutralization capacity of rainwater in the catchment. The correlation between acidic and neutralizing species was evaluated by the subsequent equation [32].

$$NF_{xi} = \frac{H+}{[SO_4^{2-}]+[NO^{3-}]} \qquad \textit{Equation 3}$$

The average ratio of H^+/ (NO_3^- + SO_4^{2-}) measured 0.07 indicates that 93% of the acidity was neutralized in the rainwater during the study period. According to the study conducted in the Kothi, North-Western Himalaya reported that almost 96 % of rainwater was neutralized [21]. The result indicates that rainwater is less acidic in Western Himalayas, particularly in the Shaune Garang catchment than in North-Western Himalaya. Also, a study in Pune and Delhi reported that the average H+/ (NO_3^- + SO_4^{2-}) ratio was 0.02 and 0.08, demonstrating that 98% and 92% of the acidity in rainwater was defused by alkaline species [33].

The average ratio of (NO_3^- + Cl^-) / (SO_4^{2-}) was measured as 2.38, indicating the higher value compared to North-Western Himalaya, mainly due to the insignificant amount of nitric and hydrochloric acid in rainfall. However, in the case of North-Western Himalaya, the ratio is slightly lower because of sulfuric acid [21]. The equal ratio of NO_3^- / SO_4^{2-} was measured 0.97 ± 0.60, which suggests the contribution to the acidity in rainwater is dominated by nitric acid and Sulphuric acid. The equal ratio of (Ca^{2+} + NH_4^+ / NO_3^- + SO_4^{2-}) is mainly used to evaluate the extent of human activity in water chemistry. All the ionic ratios of the observed ionic concentration discussed in this section in the rainwater from Shaune Garang catchment are summarized in **Table S2**. The plot (Figure 4a) between Ca^{2+} + NH_4^+ against NO_3^- + SO_4^{2-} shows the positive correlation of all data set throughout the study period and linear spread beyond the 1:1 equiline with a ratio ranging from 0.48 to 2.73 with the average equivalent value of 1.31 ± 0.51. The result indicates that NH_4^+ and Ca^{2+} ions are key factors in neutralizing acidity in rainwater through $CaSO_4$ and $(NH_4)_2SO_4$. The scatter plot between Ca^{2+} and HCO_3^- has been shown in Figure 4b. It is imperative from the figures that there is a large variation between Ca^{2+} and HCO_3^-. In rainwater, the ionic concentration of Ca^{2+} is much greater than HCO_3^- in rainwater during the study. The ratio of NH_4^+/NO_3^- extended from 0.42 to 1.00 with the mean value of 0.81 ± 0.21 and the ratio of NH_4^+/ SO_4^{2-} ranged from 0.21 to 1.46 with the mean value of 0.73 ± 0.38 signifies the dominancy of compounds NH_4NO_3 over $(NH_4)_2SO_4$ in the atmosphere [34]. Furthermore, the result from the ionic composition illustrates that the ammonium nitrate is leading over ammonium sulphate composites in the Shaune Garang catchment during the study period [35].

Neutralization Potential

The factor of acidic and neutralization potential is a significant sign of understanding rainwater's chemical behavior. The difference between rainwater's acid and neutralization potential describes the responsible factors to the entire mechanism in the process. Acid potential (AP) is the summation of Nitrate (NO_3^- and non-sea salt (NSS) Sulphate (SO_4^{2-}) concentration and neutralization potential (NP) is the sum of Ca^{2+}, Mg^{2+}, and K^+ in the rainwater. The ratio of Acid potential (AP) and neutralization potential (NP) clarify the dominancy of such factors within the system. The ratio of AP/NP measured as (0.74) less than 1 during the study period in the rainwater, indicating that neutralization potential dominates the acidic potential in the Shaune Garang catchment. In addition, the atmospheric neutralization potential of the chemical constituents in rainwater samples can be estimated through the Neutralizing Factors (NF) for the specific parameters. The neutralization factor (NF) measures how well acidic components are neutralized by crustal elements and ammonium ions. Alkaline particles serve a crucial function in modulating the acidity of RW during wet deposition [36]. The two main neutralizing sulfuric and nitric acid agents are calcium and ammonium. The primary supply of calcium is soil dust, whereas the primary source of ammonium is combustion procedures. By computing neutralization factors, the potential of Ca^{2+} and Mg^{2+} in neutralization has been established [37]. Neutralization factors

can be used to evaluate the ability of key alkaline ions in rainfall to be neutralized (NF). The following equation is used to compute the neutralization factors for ions.

$$NF_{(x)} = \frac{[x]}{NO_3^- + SO_4^{2-}}$$

Equation 4

Where: [X] is the concentration of the major ions (Ca^{2+}, Na^+, K^+, $Mg^{2+,}$ and NH_4^+) expressed in µeq/L.

The Neutralization factor, which was dominant cations like Ca^{2+}, Na^+, K^+, $Mg^{2+,}$ and NH_4^+ in the rainwater of Shaune Garang catchment, was measured as 0.85, 0.63, 0.15 0.34, and 0.39 respectively. The results suggest that the calcium ion (Ca^{2+}) in rainwater is a major controlling neutralizing agent, and potassium is minimum. The particulate matter in the rainwater, which is high in Ca^{2+} carbonates or bicarbonates, buffers the acidity of cloud-water, which is widespread in India [38-39]. These findings reveal that Ca^{2+} and Na^{2+} ions, together with NH_4^+ ions are the primary neutralization components with the minimal role of K^+ in rainfall of Shaune Garang catchment. **Table S3** shows similar observations on rainwater neutralizing capacity from several parts of India. The neutralization factor from the previous study demonstrated that the maximum neutralizing capability in rainwater was calcium (Ca^{2+}) and ammonium ions (NH_4^+) from different parts of India.

Contribution of Sea-salt and non-sea-salt

An effort was made to study the contribution of various ions in rainwater from sea salt (SS) and non-sea salt (NSS). The input of sea salt and non-sea salt to essential ions in rainwater was assessed by relating the Cl^-/Na^+ ratio in rainwater to saltwater (**Table S4**). On the other side, the NSS input was calculated by subtracting SS from the total measured ion. The measured ratio of Cl^-/Na^+ (1.14) was less than the observed seawater ratio (1.16), showing that sources of sea salt considerably impact the Cl in rainwater at the Shaune Garang area. Furthermore, increased K^+/Na^+, Mg^{2+}/Na^+, $Ca^{2+}/Na^{+,}$ and SO_4^{2-}/Na^+ ratios suggest the potential input of additional sources such as soil and nonmarine. The high SO_4^{2-} values compared to the seawater ratio in the catchment indicate a significant anthropogenic influence. Based on the relative ratios of the major ions, the probable compound formations include NaCl, $CaSO_4$, $MgSO_4$, $MgCl^2$, HNO_3, NH_4SO_4, and $(NH_4)_2SO_4$ [17 23]. The predominant ionic species in rainwater are thought to indicate the proportional effect of natural and anthropogenic sources. Natural sources include alkaline and insoluble components of mineral aerosols from the earth's crust and seas. The influences from volcanic sources are insignificant at the sample site. The enrichment factor (EF) was calculated using Na+ as the reference element.

$$EF_{(XI)} = \frac{(XI)/\ Na\ (raiwater)}{XI/Na(seawater)}$$

Equation 5

where xi is the required major ion and Xi/Na (seawater) is the seawater ratio.

The EF unity infers no enrichment and, as a result, no input from any source other than seawater. EF values greater than one, on the other hand, indicate enrichment of a specific ion relative to non-sea salt sources. It was discovered that the EF of all major ions (Mg^{2+}, K^{+}, Ca^{2+}, and SO_4^{2-}) was more than one, specifying an important input from sources other than sea salt, i.e., soil and anthropogenic sources in the catchment. The result shows that the only enrichment value of Cl^{-} is less than 1, indicating that around 97.2 % and 1.73 % come from marine and nonmarine sources, respectively. The enrichment factor of Shaune Garang, compared with the other previous studies in India, indicates that the EF value of Kothi, Himachal Pradesh (Table S5) is very similar to the present study. Therefore, it is verified that the predominance of nonmarine contributions influences the Shaune Garang catchment. However, our observation compared with the previous research from Nainital, Uttarakhand indicates that the chemical configuration of rainwater in the Himalayan region is affected by both natural and anthropogenic sources.

Air mass trajectory analysis

Particulate matter concentrations have risen rapidly in developing countries such as India because of high emissions from a variety of human-caused events [40-41]. The researchers studied the influence of aerosols on the earth's radiation budget, weather, rainfall, and cloud formation [42-43]. Aerosol emissions are to blame for rising regional temperatures and have been identified as a key factor in the melting of the Hindu Kush-Himalayan-Tibetan glaciers [44]. The Himalayan region has also been affected by heating caused by another amalgamation of solar energy due to aerosol brown cloud [45]. It can similarly decrease the albedo of snow and glaciers, leading to enhanced melting because of the accumulation of radiation-absorbing aerosols on them. Previous study [46] has estimated that the annual average melting of Himalaya reached from 0.7-0.85 m w.e. per annum at Lahaul/Spiti glaciers during 1999-2004. Moreover, the backward air trajectory modeling significantly showed the impacts up to the Mt. Everest region due to high aerosol emissions from the North-west region. The air mass back trajectories are critical for determining the potential transportation paths of air mass to the station. To understand the other pollution sources, air mass back trajectories were computed for the study area using the NOAA Hybrid Single-Particle Lagrangian Integrated Trajectory (HYSPLIT) model [47]. GDAS (Global Data Assimilation System) data was used to generate three-dimensional back trajectories [48] for the

monitoring location in Shaune Garang glacier on precipitation days. During July, 80% of air parcels were coming from the northwest direction at relatively higher levels which may carry various air pollutants to the study locations. The speed of the wind and atmospheric boundary layer's height play an essential part in the diurnal difference of pollutant concentrations and dispersion. The measured ion concentration was approximately two and a half times higher than the air masses passing from the southwest. The bulk of air masses are arriving from the west (the Mediterranean Sea or the mid-west Atlantic Ocean), also known as western disturbances, according to the research. These air masses pass over the Persian Gulf, Iran, Afghanistan, and Pakistan, bringing torrential rainfall to the western Himalayas. Along the dust track, long-distance dust movement interacts with anthropogenic emissions, raising local particulate matter concentrations [49]. The back trajectory analysis (**Figure 5**) clearly shows that in July, 60% of the air parcels were coming from the Arabian Sea and Bay of Bengal, with the remainder coming from the northwest direction of India. The Arabian Sea disturbance resulted in a significant reduction in ion mass concentrations.

Chemometric analysis

The correlation coefficient matrix was made among the measured chemical components in rainwater to identify the relationship between all chemical species (Table S6). The correlation analysis specifies chemical parameters such as SO_4^{2-}– NO_3^-, Mg^{2+}– NO_3^-, Na^+ – SO_4^{2-}, Ca^{2+}– Cl^-, SO_4^{2-} – Cl^- and NO_3^- –HCO_3^- have a reasonable correlation. The correlation coefficients between Cl^- and SO_4^{2-} (0.50) indicate that it is influenced by crustal soil. In addition, a minimal correlation (0.22) between bicarbonate and soil-derived Ca^{2+} was observed among the ions, indicating that the contribution of these sources was influenced by soil dust containing large fractions of $CaCO_3$ originating from the same sources. The correlation among Ca^{2+} and NO_3^- was observed to be 0.44 during the study period, suggesting that soil is the most important source of nitrate in rainwater, which is present in the atmosphere in the form of $Ca(NO_3)_2$ [21]. Minor contaminants like sulfate (SO_4^{2-}) and nitrate (NO_3^-) are significantly correlated (0.67), showing their origin from the same sources. The controlling contribution factor of SO_4^{2-} and NO_3^- in acid formation was nearly 54.64 % and 45.38 % respectively in the catchment. Therefore, the findings demonstrate that the high concentrations in the Himalayan area are thought to be caused by airborne primary and secondary particle movement. Apart from this, a good correlation (0.56) observed between Na^+ and Cl^- suggests that most of Na^+ and Cl^- components originated from marine sources and were transported with air masses. However, the ionic ratio of Cl^-/Na^+ in the rainwater compared to the seawater ratio in the previous section (Table S4) indicates a part of chloride from other emission sources.

To identify potential sources of ionic species in rainwater, factor and principal component were used. The correlation matrix was exposed to Bartlett's Sphericity test, which yielded 2 (critical) = 84.93, which was more significant than the critical value 2 (critical = 30.61; df- 45 and p-value 0.0001 with significance level 0.05). Following varimax rotation, factor extraction with an Eigenvalue greater than 1 was used to perform principal component analysis (PCA). The Pearson correlation coefficient between the measured

chemical components in rainwater supported the factor components. In principal component analysis, the data were exposed to a Varimax rotation, which optimizes the variance to generate a pattern of loadings on each factor that is as different as possible, allowing for easier interpretation. Factor loadings represent the correlations of each variable with the factor. In this study, four factors were identified, and each variable was assigned a loading with each factor. When the loading of each variable was determined to be greater than 0.50, the significant loading was considered. Table 1 summarizes the loadings with the variance extracted by the factors (Eigenvalue).

Table 1

Principal components (PCs) loading for selected physic-chemical parameters in rainwater.

1	F1	F2	F3	F4
pH	**-0.672**	0.306	0.148	-0.069
EC	0.276	0.648	-0.296	-0.458
Na^+	0.299	0.763	0.101	-0.078
K^+	-0.072	-0.545	0.699	0.079
Ca^{2+}	**0.771**	-0.230	0.277	-0.072
Mg^{2+}	**-0.541**	0.452	-0.059	0.623
Cl^-	**0.596**	0.362	0.389	0.427
SO_4^{2-}	0.423	0.646	0.480	-0.121
NO_3^-	**-0.685**	0.534	0.250	0.007
HCO_3^-	**-0.643**	-0.091	0.480	-0.470
Eigenvalue	2.924	2.492	1.363	1.037
Variability (%)	27.894	24.981	14.640	10.857
Cumulative (%)	27.894	52.875	67.515	78.373

The four rotated principal components (PC) were formed during the analysis, including Eigenvalues, percentage of variation, and cumulative percent variability**.** All the principal components (PC) with its Eigenvalues are considered more than to assess the governing factor in the rainwater. In a scree plot (Figure 6) in the PCA, the cumulative variability was measured as 78.3%, including four-component (PC1 explained 27.89%, PC2 explained 24.98 % PC3 explained 14.64 % PC4 explained 10.85 %). PCA generated four significant factors clarifying 78.37 % of the total data variance. However, Factor 1 explains 27.89 % of the data variance and displays a strong optimistic loading for Ca^{2+} and Cl^-. High loadings of Ca^{2+} NO_3^-

and moderate loading of SO_4^{2-} signify that the most important sources of these ions are the burning of fossil fuel and soil dust.

In addition, the first two PC loadings were drawn to understand and interpret the grouping and association amongst the variables. Results clarify that (Factor I and II) explain 52.87 % of the total variance (Figure S3a and S3b). High loadings of a chemical constituent such as Cl^-, Ca^{2+}, Mg^{2+}, NO_3^- and HCO_3^- demonstrate the natural sources, sea, and soil. Factor II comprises NO_3^-, K^+, and SO_4^{2-}, indicating that the sources of these chemical constituents from vehicular emissions and biomass burning. Although Na^+ and Cl^- generally come in the form of sea salt but give the impression of the same factor. Even if SO_4^{2-} is not originated from the sources of soil or the sea, it seems that it might be due to the marine wind containing SO_4^{2-} and Ca^{2+} [19]. Apart from this, as most of the Mg^{2+} originates from the sea source thus, it appears in this factor. The SO_4^{2-} over the study region is primarily due to inadequate fuel burning, fertilizer uses, thermal power plants, refineries, and long-range transport.

Comparison of ion concentrations in rainwater at higher altitude regions

The ionic concentration of the rainwater of Shaune Garang catchment was compared with the ionic concentration of rainwater from several study areas around the world, such as China, Nepal, Tibet, and India (Figure 7). However, it is imperative to emphasize that the most relevant parameters which accelerate the formation of acid rain are NO_3^- and SO_4^{2-}. In Shaune Garang catchment, high intensities of SO_4^{2-} (23.83 μeq/l) and NO_3^- (18.75 μeq/l) were observed during the study period. Therefore, these two parameters are the primary inorganic ions formed from $SO_4^{2-}$and NO_3^- gases during the precipitation event, emitted from different sources such as vehicular emission at high altitudes [50]. The concentration of NO_3^- in the sampling area (18.75 μeq/l) surpassed the concentrations observed in the study area of Kathmandu (12.75 μeq/l), Dhunche (10.70 μeq/l), Dimsa (8.52 μeq/l), Gosainkunda (4.40 μeq/l), Southern Everest region (0.01 μeq/l), Northern Everest region (1.10 μeq/l), Nam co Tibet (10.30 μeq/l), Lhasa (2.0 μeq/l), Southern Tibet plateau (2.33 μeq/l), Nainital, Uttrakhand (11.9 μeq/l). Therefore, with the known fact that NO_3^- is a pioneer gas for forming acid rain, it produces nitric acid with soil interaction, causing high nitrification with the metal's mobilization. Consequently, SO_4^{2-} originates primarily from vehicle traffic and industrial effluence. In this study, the concentration of Na^+ (27.66 μeq/l) and Cl^- (31.28μeq/l) were observed low compared to the study area Nainital, Uttrakhand, where Na^+ was observed as 49.8 μeq/l and Cl^- was 67.3 μeq/l. The ratio (Cl^- /Na^+) was calculated for the study area and observed the ratio of Shaune Garang catchment was 1.13, indicating the origin in marine sources. According to the European Union, Air Pollution Study Group recommends that the Na^+/Cl^- ratio between 0.5 and 1.5 indicate a marine source. In the Shaune Garang catchment, values are significantly closer to the range, and it is possible that the Na^+ also might have a continental origin. The concentration of HCO_3^- (8.09 μeq/l) in the Shaune Garang catchment has been lower than the reported values of other locations. This result indicates that the HCO_3^- ion is also significantly present in rainwater samples of Shaune

Garang catchment, and it is largely imitative from soil resuspension and limestone use around the study area [51-52]. Even though the concentration of HCO_3^- in Lhasa is very high as compared to another study, this might be due to high limestone exploitation at a particular study area. Apart from these parameters, Mg^{2+} (13.98 µeq/l) was observed high compared to another study, however, K^+ (6.56 µeq/l) and Ca^{2+} (37.13 µeq/l) were almost similar in all studies. These parameters, such as Mg^{2+}, $Ca^{2+,}$ and K^+ originate primarily from seawater, soil, and forest fires [53] and heavy agricultural and intense agricultural vehicular traffic [54].

Conclusion

The significant ionic concentration in the rainwater was measured in the Shaune Garang catchment. The pH of rainwater ranged from 4.59 to 6.73 with an average value of 5.47 ± 0.69; this result suggests that the rainwater composition is influenced by anthropogenic and natural chemical constituents. Total cations and anions during the study were observed 169.4 ± 40.1 µeq/l, and the abundance of ions show a trend as $C1^- > SO_4^{2-} > NO_3^- > HCO_3^-$ for anions and $Ca^{2+} > Na^+ > Mg^{2+} > K^+$ for cations in the rainwater. Although the average ratio of acidic species (SO_4^{2-} / NO_3^-) was measured as 1.20, suggesting the contribution of SO_4^{2-} and NO_3^- in the precipitation. Apart from this, Neutralization factors for Ca^{2+} and Mg^{2+} in the rainwater of Shaune Garang catchment were 0.87, 0.32, indicating that both ionic species are an essential factor for neutralization. Air mass trajectory analysis revealed that most air masses are coming from the west (the Mediterranean Sea or the mid-west Atlantic Ocean). Long-range transport of dust mixes with anthropogenic emissions along the dust track, enhancing local particulate matter concentrations. It is observed that 60% of the air parcels reaching the Shaune Garang Catchment were coming from the Arabian Sea and Bay of Bengal in July and the rest from the northwest direction of India. A significant amount of reduction in mass concentrations of ions was measured due to Arabian Sea disturbance. Based on the rigorous analysis, the present study concludes that rainwater composition in the pristine Himalayas is largely exaggerated by anthropogenic and natural sources of other regions due to long-range transference.

Study Area

The research study area is in the Baspa Basin of the Kinnaur district of Himachal Himalaya. Meltwater from the Shaune Garang glacier flows into the Baspa River in Sangla Valley. The catchment's total area is approximately 60 km^2, while the catchment's area above the discharge gauging site is approximately 38.13 km^2 [55-58]. Himachal Pradesh's Shaune Garang glacier basin is located between 31o16'45" N and 31o18' N and 78o18'30" E and 78o22' E". Climatic parameters are the primary regulators of the mountain and glacier dynamics. From May to September, the region is subjected to ablation [55].

This catchment receives rainfall from the westerlies in winter and the monsoon in summer, with summer precipitation predominating [59]. The winter rainfall in this region is received through the Western Disturbance (WD) [60]. An excessive inconsistency in rain and snowfall patterns has been reported in the

Himalayas with varying amounts of precipitation of 100 to >1600 cm [61] depending on the terrain and local climatic conditions. The contribution of monsoon is more considerable, mainly in the eastern Himalayas, and reduces towards the western Himalayas. In contrast, the westerly contributes more to the western parts of the Himalayas and declines towards the eastern. The rocks of this region resemble the Higher Himalayan Crystalline. It contains pelitic and psammopelitic meta-sediments having acidic and basic intrusive. Different types of granite and gneiss rocks are found in the Himalayan region and have an ordinary presence of late-stage pegmatitic veins. This also has light grey-green colored feldspar. Rohtang gneiss is the principal constituent of the Himalayan glacier's area. Chalcopyrite is also obtained in lateral morainic deposits of the Himalayas. The study area has major geologic components of the "Rakcham group of granite" [62]. The study area is presented in Figure 8.

Water sample collection and chemical analysis

The study of cations and anions of rainwater was performed in Shaune Garang catchment in the ablation season (June to September) in 2017. Sixteen samples of rainwater were collected throughout the study period in the catchment. Rainwater samples were collected in a rain collector made of a polyethene bucket at elevations ranging from 3500 to 4500 m asl. The sample sites were divided into five zones in the catchment. Before collecting rainwater samples, the bucket was cleansed and rinsed twice with distilled water. Rainwater samples were filtered using 0.45µm filter paper into a prewashed cleaned polypropylene bottle. After collecting samples, the pH and EC were observed on-site by a handheld multi-parameter instrument (HANNA). All rainwater samples were kept at 4°C until analysis. Atomic Absorption Spectroscopy was used to determine the major cations (Ca^{2+}, Mg^{2+}, K^{+}, Na^{+}). For Ca^{2+}, Mg^{2+}, K^{+}, and Na^{+}, the instrument has a precession limit of 0.05 ppm. Ion Chromatograph (PERKIN ELMEWR), Dionex ICS 900, USA, with a precision of 0.1 ppm, was used to analyze the anions (Cl^{-}, SO_4^{2-}, and NO_3^{-}). The sample analysis procedures followed the [63] guidelines. The methodical accuracy was maintained using known standard solutions of ionic radicals. The NOAA Air Resources Laboratory's Hybrid Single-Particle Lagrangian Integrated Trajectory (HYSPLIT) model (http://www.arl.noaa.gov/ready/hysplit4.html) was used to access the transportation of air parcels at the Shaune Garang catchment.

Declarations

Acknowledgement

I would like to acknowledge USAID funded project entitled “Contribution to High Asia Runoff from Ice and Snow” (CHARIS) under the collaboration of University of Colorado, Boulder, USA for financial support during my PhD. The support of the Department of Science and Technology DST/CCP/NHC/159/2018(G), dated March 28, 2019, through the research project on Naradu glacier sanctioned to Prof. Rajesh Kumar (PI of the project) is thankfully acknowledged.

Data and materials availability: The datasets used and/or analyzed during the current study are available on reasonable request from the corresponding author.

Author contribution: Ramesh Kumar and Atar Singh: Collected the data, performed the analysis, wrote the paper. Rajesh Kumar, Mohammad Arif, and Pankaj Kumar: Supervising, checking the manuscript. Anupma Kumari: Performed the laboratory analysis.

Declaration

Ethics approval and consent to participate are not required.

Consent for publication: Not required.

Competing interests: The authors declare that they do not have any competing interests.

References

1. Immerzeel, W.W., Lutz, A.F., Andrade, M. *et al.* Importance and vulnerability of the world's water towers. *Nature***577,** 364–369 (2020). https://doi.org/10.1038/s41586-019-1822-y.
2. Benn, D. I. *et al.* Response of debris-covered glaciers in the Mount Everest region to recent warming, and implications for outburst flood hazards. *Earth-Science Reviews* 114, 156–174 (2012). https://doi.org/10.1016/j.earscirev.2012.03.008.
3. Lelieveld, J. *et al.* Effects of fossil fuel and total anthropogenic emission removal on public health and climate. *Proceedings of the National Academy of Sciences***116,** 7192–7197 (2019). https://doi.org/10.1073/pnas.1819989116.
4. Keresztesi, Á. *et al.* Spatial and long-term analysis of rainwater chemistry over the conterminous United States. *Environmental Research* 188, 109872 (2020). https://doi.org/10.1016/j.envres.2020.109872.
5. Obaidy, A., Joshi, H. Chemical composition of rainwater in a tropical urban area of northern India. *Atmospheric Environment* 40:6886–6891 (2006). https://doi.org/10.1016/j.atmosenv.2005.01.031.
6. Health Effects Institute. State of Global Air 2019. Special Report. Boston, *MA: Health Effects Institute.* (2019).
7. Choi, B.Y., Yun, S.T., Yeom, G.I., Kim, K.H., Kim, K.H., Koh, Y.K. Spatio-temporal variation of pH and ionic concentrations in precipitation: interaction between two contrasting stationary sources affecting air quality. *Geosciences Journal* 12(3), 205–213 (2008). https://doi.org/10.1007/s12303-008-0021-x.
8. Singh, A. K., Mondal, G. C., Kumar, S., Singh, K. K., Kamal, K. P., Sinha, A. Precipitation Chemistry and Occurrence of Acid Rain Over Dhanbad, Coal City of India. *Environmental Monitoring and Assessment* 125(1-3) 99–110. (2006). https://doi.org/10.1007/s10661-006-9243-4.
9. Alves, D. D. *et al.* Chemical composition of rainwater in the Sinos River Basin, Southern Brazil: a source apportionment study. *Environmental Science and Pollution Research* 25(24), 24150–24161 (2018). https://doi.org/10.1007/s11356-018-2505-1.

10. Bhaskar, V. V., Rao, P. S. P. Annual and decadal variation in chemical composition of rainwater at all the ten GAW stations in India. *Journal of Atmospheric Chemistry* 74(1), 23–53. (2016). https://doi.org/10.1007/s10874-016-9339-3.
11. Budhavant, K. B., Rao, P. S. P., Safai, P. D., Granat, L., Rodhe, H. Chemical composition of the inorganic fraction of cloud-water at a high altitude station in West India. *Atmospheric Environment* 88, 59–65 (2014). https://doi.org/10.1016/j.atmosenv.2014.01.039.
12. Das, N., Das, R., Chaudhury, G. R., Das, S. N. Chemical composition of precipitation at background level. *Atmospheric Research* 95(1), 108–113. (2010). https://doi.org/10.1016/j.atmosres.2009.08.006.
13. Gong, W., Stroud, C., Zhang, L. Cloud processing of gases and aerosols in air quality modeling. *Atmosphere* 2 (4), 567e616 (2011). https://doi.org/10.1016/j.atmosres.2009.08.006.
14. Kajino, M., Aikawa, M. A model validation study of the washout/rainout contribution of sulfate and nitrate in wet deposition compared with precipitation chemistry data in Japan. *Atmospheric Environment* 117, 124e134 (2015). https://doi.org/10.1016/j.atmosenv.2015.06.042.
15. Arimoto, R*. et al.* Chemical composition of atmospheric aerosols from Zhenbeitai, China, and Gosan, South Korea, during ACE-Asia. *Journal of Geophysical Research* 109(D19) (2004). https://doi.org/10.1029/2003jd004323.
16. Tiwari, S., Kulshrestha, U.C., Padmanabhamurtyc, B. Monsoon rain chemistry and source apportionment using receptor modeling in and around National Capital Region (NCR) of Delhi, India. *Atmospheric Environment* 41, 5595–5604 (2007). https://doi.org/10.1016/j.atmosenv.2007.03.003.
17. Mouli, P.C., Venkata, M.S., Jayarama, R.S. Rainwater chemistry at a regional representative urban site: influence of terrestrial sources on ionic composition. *Atmospheric Environment* 39, 999–1008 (2005). https://doi.org/10.1016/j.atmosenv.2004.10.036.
18. Kulshrestha, U.C., Granat, L., Engardt, M., Rodhe, H. Review of precipitation chemistry studies in India, a search for regional patterns. *Atmospheric Environment* 39, 7403–7419 (2005). https://doi.org/10.1016/j.atmosenv.2005.08.035.
19. Budhavant, K. B., Rao, P. S. P., Safai, P. D., Ali, K. Chemistry of Monsoon and Post-Monsoon Rains at a High Altitude Location, Sinhagad, India. *Aerosol and Air Quality Research* 9(1), 65–79 (2009). https://doi.org/10.4209/aaqr.2008.07.0033.
20. Shrestha, A. B., Wake, C. P., Dibb, J. E., Whitlow, S. I. Aerosol and Precipitation Chemistry at a Remote Himalayan Site in Nepal. *Aerosol Science and Technology* 36(4), 441–456 (2002). https://doi.org/10.1080/027868202753571269.
21. Tiwari, S., Chate, D. M., Bisht, D. S., Srivastava, M. K., Padmanabhamurty, B. Rainwater chemistry in the North Western Himalayan Region, India. *Atmospheric Research* 104-105, 128–138 (2012). https://doi.org/10.1016/j.atmosres.2011.09.006.
22. Roy, A. et al. Precipitation chemistry over urban, rural and high altitude Himalayan stations in eastern India. *Atmospheric Research* 181, 44–53 (2016). https://doi.org/10.1016/j.atmosres.2016.06.005.

23. Bisht, D. S. *et al.* Chemical characterization of rainwater at a high-altitude site “Nainital” in the central Himalayas, India. *Environmental Science and Pollution Research* 24(4), 3959–3969 (2016). https://doi.org/10.1007/s11356-016-8093-z.
24. Akpo, A.B. *et al.* Precipitation chemistry and wet deposition in a remote wet savanna site in West Africa: Djougou (Benin). *Atmospheric Environment* 115, 110–123 (2015). https://doi.org/10.1016/j.atmosenv.2015.04.064.
25. Khwaja, H. A., Husain, L. Chemical characterization of acid precipitation in Albany, New York. *Atmospheric Environment* 24:1869–1882 (1990). https://doi.org/10.1016/0960-1686(90)90519-S.
26. Ozlem, I. Investigation of 8 years long composition record in the eastern Mediterranean precipitation. MS thesis. Department of Environmental Engineering, *Middle East Technical University, Ankara* (2006).
27. Kaskaoutis, D. G. *et al.* Effects of crop residue burning on aerosol properties, plume characteristics, and long-range transport over northern India. *Journal of Geophysical Research: Atmospheres* 119(9), 5424–5444 (2014). https://doi.org/10.1002/2013jd021357.
28. Tiwari, S. et al. Nature and Sources of Ionic Species in Precipitation across the Indo-Gangetic Plains, India. *Aerosol and Air Quality Research* 16(4), 943–957 (2016). https://doi.org/10.4209/aaqr.2015.06.0423.
29. Xiao, J. Chemical composition and source identification of rainwater constituents at an urban site in Xi’an. *Environmental Earth Sciences* 75(3) (2016). https://doi.org/10.1007/s12665-015-4997-z.
30. Kumar, R., Rani, A., Singh, S.P., Kumari, K.M., Srivastava, S.S. A long term study on chemical composition of rainwater at Dayalbagh, a suburban site of semiarid region. *Journal of Atmospheric Chemistry* 41: 265–279 (2002). https://doi.org/10.1023/A:1014955715633.
31. Mukherjee, S. *et al.* Seasonal variability in chemical composition and source apportionment of sub-micron aerosol over a high altitude site in Western Ghats, India. *Atmospheric Environment* 180, 79–92 (2018). https://doi.org/10.1016/j.atmosenv.2018.02.048.
32. Balasubramanian, R., Victor, T., Chun, N. Chemical and statistical analysis of precipitation in Singapore. *Water, Air, and Soil Pollution* 130: 451–456, (2001). https://doi.org/10.1023/A:1013801805621.
33. Rao, P. S. P. *et al*. Sources of chemical species in rainwater during monsoon and non-monsoonal periods over two mega cities in India and dominant source region of secondary aerosols. *Atmospheric Environment* 146, 90–99 (2016). https://doi.org/10.1016/j.atmosenv.2016.06.069.
34. Seinfeld, J.H. Atmospheric chemistry and physics of air pollution.1986.
35. Parmar, R. S., Satsangi, G. S., Lakhani, A., Srivastava, S. S., Prakash, S. (2001). Simultaneous measurements of ammonia and nitric acid in ambient air at Agra (27°10'N and 78°05'E) (India). *Atmospheric Environment* 35(34), 5979–5988 (2001). https://doi.org/10.1016/s1352-2310(00)00394-0.
36. Rodhe, H., Dentener, F., Schulz, M. The Global Distribution of Acidifying Wet Deposition. *Environmental Science and Technology* 36(20), 4382–4388 (2002).

https://doi.org/10.1021/es020057g.

37. Kulshrestha, M. J., Kulshrestha, U. C., Parashar, D. C., Vairamani, M. Estimation of SO_4 contribution by dry deposition of SO_2 onto the dust particles in India. *Atmospheric Environment* 37(22), 3057–3063 (2003). https://doi.org/10.1016/s1352-2310(03)00290-5.
38. Shukla, S. P. and Sharma, M. Neutralization of rainwater acidity at Kanpur, India. *Tellus B* 62(3) (2010). https://doi.org/10.3402/tellusb.v62i3.16523.
39. Budhavant, K. B., Rao, P. S. P., Safai, P. D., Ali, K. Influence of local sources on rainwater chemistry over Pune region, India. *Atmospheric Research* 100(1), 121–131 (2011). https://doi.org/10.1016/j.atmosres.2011.01.004.
40. Adhikary, B. *et al.* Characterization of the seasonal cycle of south Asian aerosols: A regional-scale modeling analysis. *Journal of Geophysical Research* 112(D22) (2207). https://doi.org/10.1029/2006jd008143.
41. Carmichael, G. R. *et al.* Asian Aerosols: Current and Year 2030 Distributions and Implications to Human Health and Regional Climate Change. *Environmental Science & Technology* 43(15), 5811–5817 (2009). https://doi.org/10.1021/es8036803.
42. Wang, W. et al. Chemical compositions of fog and precipitation at Sejila Mountain in the southeast Tibetan Plateau, China. *Environmental Pollution* 253, 560–568 (2019). https://doi.org/10.1016/j.envpol.2019.07.055.
43. Ramanathan, V. *et al.* Atmospheric brown clouds: Hemispherical and regional variations in long-range transport, absorption, and radiative forcing. *Journal of Geophysical Research* 112(D22) (2007). https://doi.org/10.1029/2006jd008124.
44. Ramanathan, V., Carmichael, G. Global and regional climate changes due to black carbon. *Nature Geoscience* 1, 221–227 (2008). https://doi.org/10.1038/ngeo156.
45. Chand, D., Wood, R., Anderson, T. L., Satheesh, S. K., Charlson, R. J. Satellite-derived direct radiative effect of aerosols dependent on cloud cover. *Nature Geoscience* 2(3), 181–184 (2009). https://doi.org/10.1038/ngeo437.
46. Berthier, E. *et al.* Remote sensing estimates of glacier mass balances in the Himachal Pradesh (Western Himalaya, India). *Remote Sensing of Environment* 108(3), 327–338 (2007). https://doi.org/10.1016/j.rse.2006.11.017.
47. Draxler, R.R., Rolph, G.D. HYSPLIT (HYbrid Single-Particle Lagrangian Integrated Trajectory) Model access via NOAA ARL READY Website (http://www.arl.noaa.gov/HYSPLIT.php). NOAA Air Resources Laboratory, College Park, MD.
48. Kanamitsu, M. Description of the NMC Global Data Assimilation and Forecast System. *Weather and Forecasting* 4(3), 335–342 (1989). https://doi.org/2.0.co;2">10.1175/1520-0434(1989)004<0335:dotngd>2.0.co;2.
49. Bhattacharjee, P. S., Prasad, A. K., Kafatos, M., Singh, R. P. Influence of a dust storm on carbon monoxide and water vapor over the Indo-Gangetic Plains. *Journal of Geophysical Research* 112(D18) (2007). https://doi.org/10.1029/2007jd008469.

50. Seinfeld, J.H., Pandis, S.N. Atmospheric Chemistry and Physics: From Air Pollution to Climate Change. 2nd Edition, John Wiley & Sons, New York. (2006).
51. Reimann, C. et al. Geochemical analysis of soil in the central Barents Region. PANGAEA (1998). https://doi.org/10.1594/PANGAEA.686641.
52. Castillo, S., Alastuey, A., Cuevas, E., Querol, X., Avila, A. Quantifying Dry and Wet Deposition Fluxes in Two Regions of Contrasting African Influence: The NE Iberian Peninsula and the Canary Islands. *Atmosphere* 8(12), 86 (2017). https://doi.org/10.3390/atmos8050086.
53. Đorđević, D., Mihajlidi-Zelić, A., Relić, D. Differentiation of the contribution of local resuspension from that of regional and remote sources on trace elements content in the atmospheric aerosol in the Mediterranean area. *Atmospheric Environment* 39(34), 6271–6281 (2005. https://doi.org/10.1016/j.atmosenv.2005.07.006.
54. Reimann, C., Caritat, P. Chemical Elements in the Environment. *factsheets for the Geochemist and Environmental Scientist* 398pp. (1998).
55. Kumar, R. *et al.* Development of a Glacio-hydrological Model for Discharge and Mass Balance Reconstruction. *Water Resources Management* 30(10), 3475–3492 (2016). https://doi.org/10.1007/s11269-016-1364-0.
56. Kumar, R., Kumar, R., Singh, A., Sinha, R.K., Kumari A. Nanoparticles in glacial meltwater. Mater Today Proc 5(3P1):9161–9166 (2018). https://doi.org/10.1016/j.matpr.2017.10.037.
57. Kumar. R et al. Dynamics of suspended sediment load with respect to summer discharge and temperatures in Shaune Garang glacierized catchment, Western Himalaya. *Acta Geophysica* 66(5), 1109–1120 (2018). https://doi.org/10.1007/s11600-018-0184-4.
58. Kumar, R. *et al*. Distribution of trace metal in Shaune Garang catchment: evidence from particles and nanoparticles. *Materials Today Proceedings* 15(3):586–594 (2019). https://doi.org/10.1016/j.matpr.2019.04.125.
59. Wulf, H., Bookhagen, B., Scherler, D. Seasonal precipitation gradients and their impact on fluvial sediment flux in the Northwest Himalaya. *Geomorphology* 118(1-2), 13–21 (2010). https://doi.org/10.1016/j.geomorph.2009.12.003.
60. Dimri, A. P. Surface and Upper Air Fields During Extreme Winter Precipitation Over the Western Himalayas. Pure and Applied Geophysics, 163(8), 1679–1698 (2006). https://doi.org/10.1007/s00024-006-0092-4.
61. Bhutiyani, M. R., Kale, V. S., Pawar, N. J. Climate change and the precipitation variations in the northwestern Himalaya: 1866-2006. *International Journal of Climatology* 30(4), 535–548 (2009). https://doi.org/10.1002/joc.1920.
62. Dutta, S., Mujtaba, S. A. I., Saini, H. S., Chunchekar, R., Kumar, P. Geomorphic evolution of glacier-fed Baspa Valley, NW Himalaya: record of Late Quaternary climate change, monsoon dynamics and glacial fluctuations. *Geological Society, London, Special Publications* 462(1), 51–72 (2017). https://doi.org/10.1144/sp462.5.
63. APHA (2005) WEF, 2005. Stand. Methods Exam Water Wastewater 21:258–259.

Figures

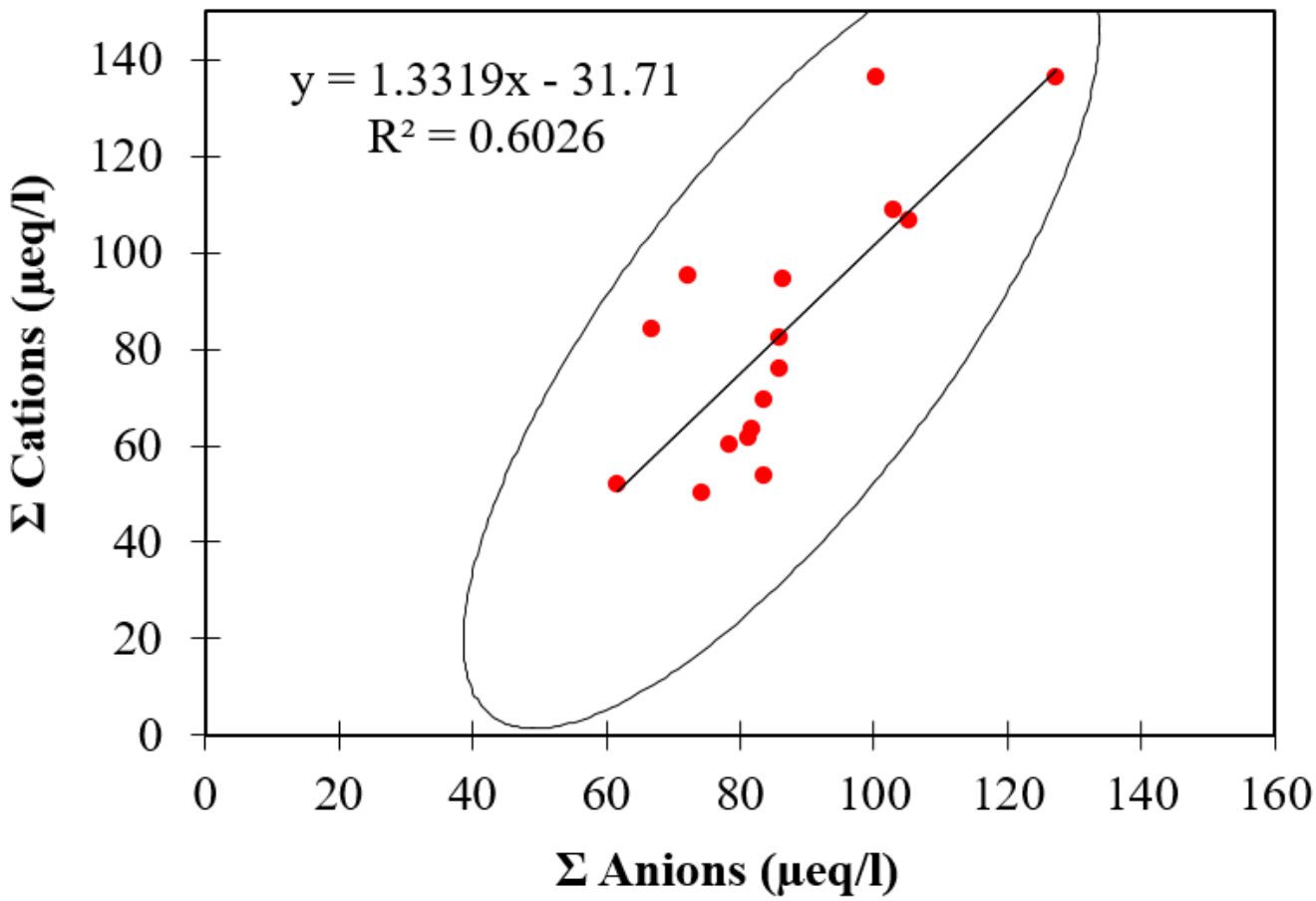

Figure 1

Correlation among the sum of anions and sum of cations during the ablation period of 2017.

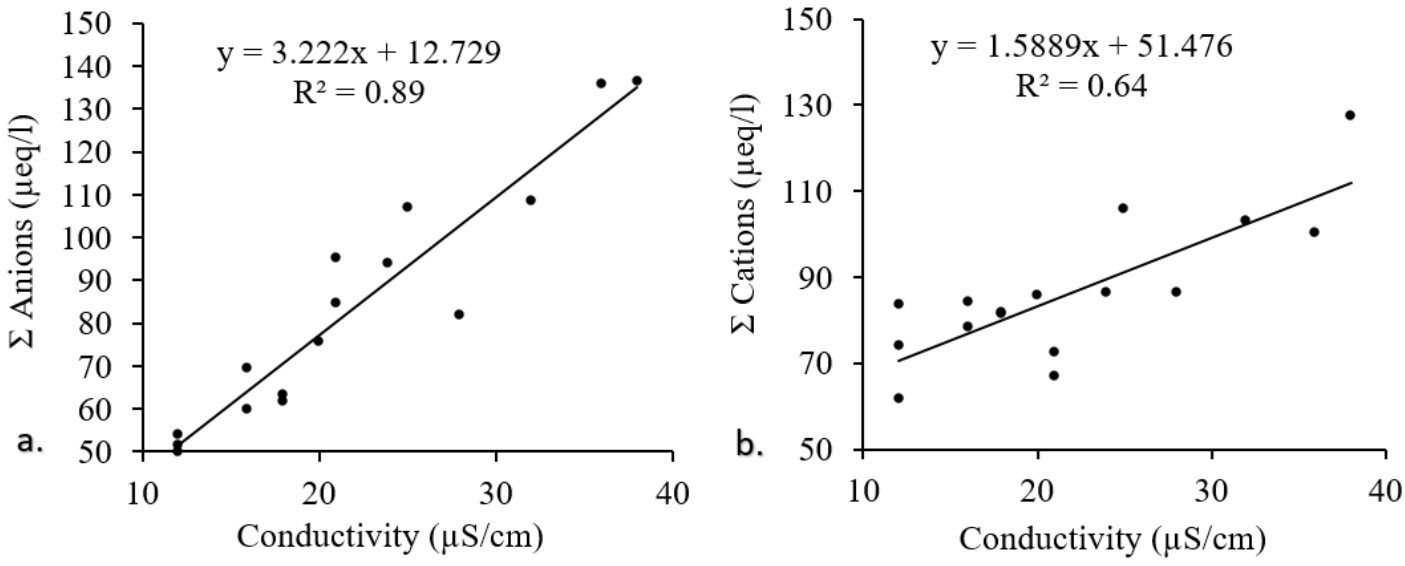

Figure 2

Scatter plot of conductivity against (a) sum of anions and (b) sums of cations.

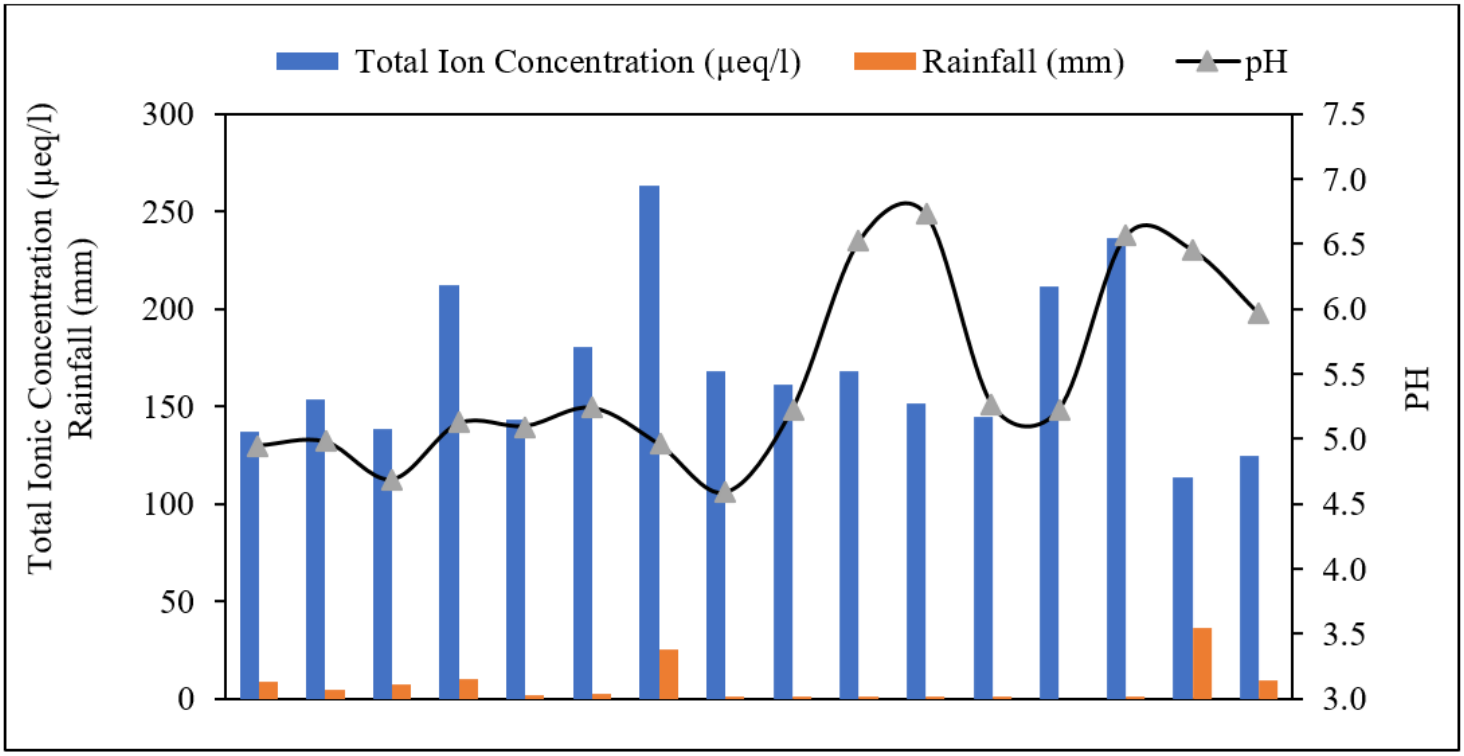

Figure 3

Average seasonal pH variations, rainfall amount, and species concentrations.

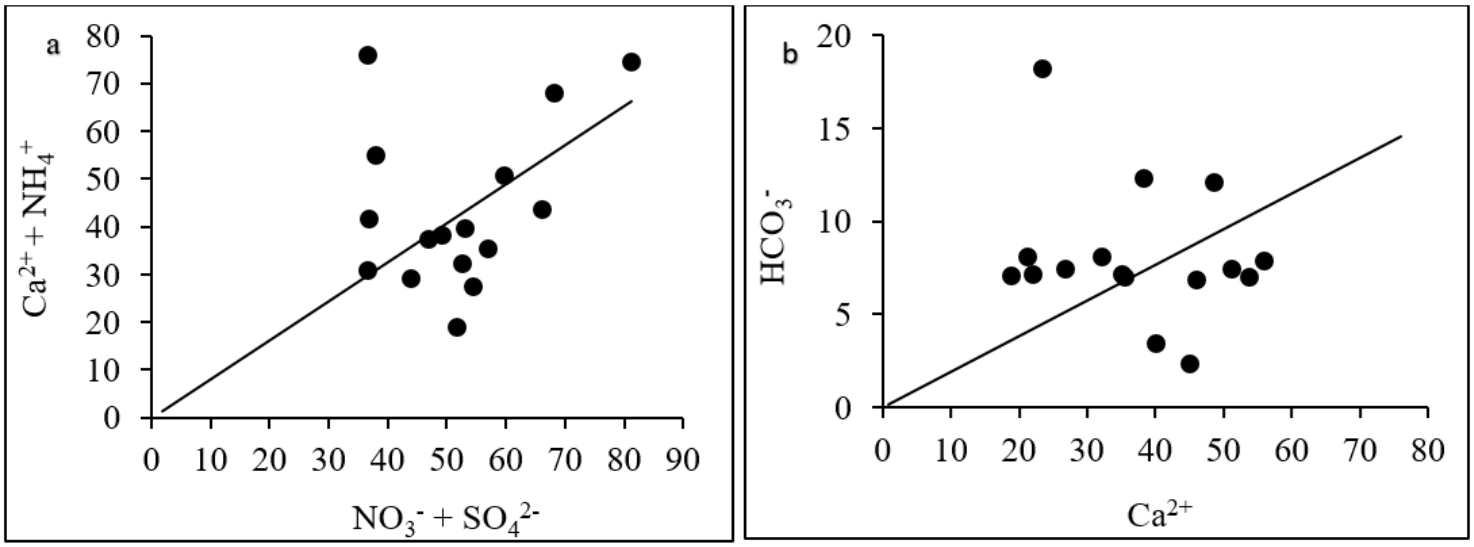

Figure 4

a. Scatter plot of Ca^{2+} + NH_4^+ against NO_3^- + SO_4^{2-} and **b**. Ca^{2+} against HCO_3^- during the study period in Shaune Garang catchment.

Figure 5

Backward trajectories at rainwater sampling site in Shaune Garang glacier catchment.

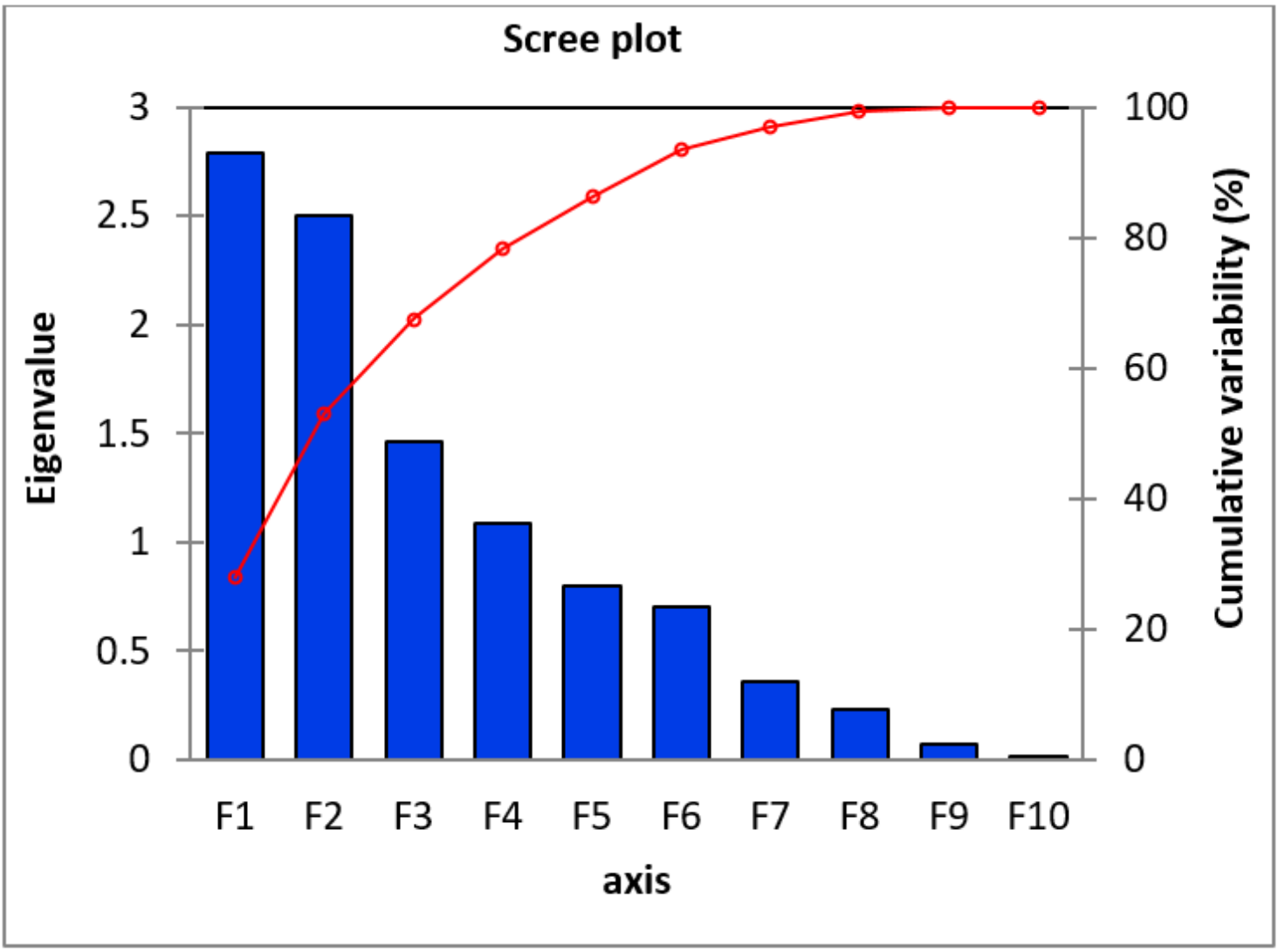

Figure 6

Scree plot graph between eigenvalue and factors

Figure 7

The average chemical constituent of rainwater from Shaune Garang catchment and its comparison with a chemical constituent of rainwater from another high-altitude region.

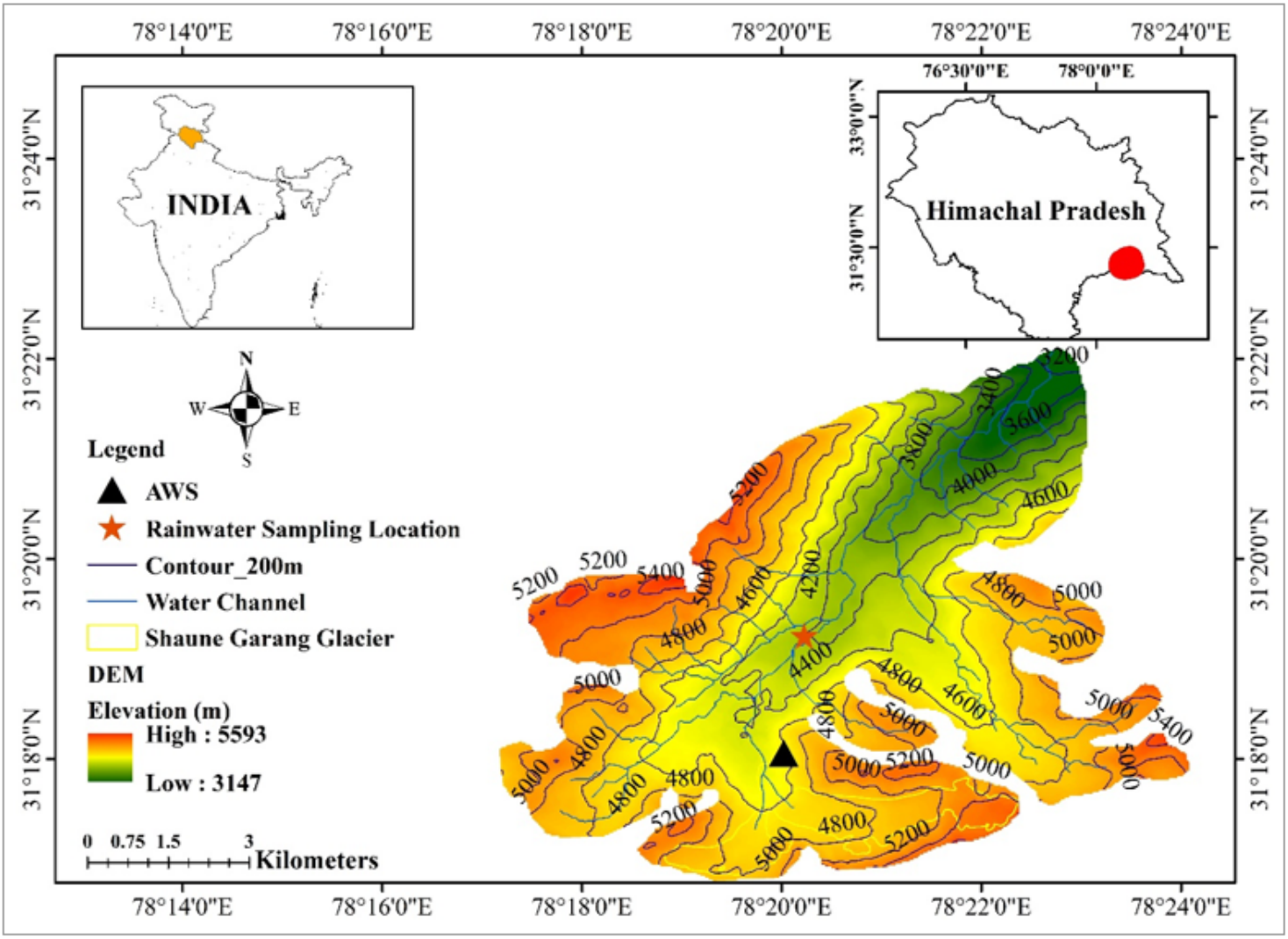

Figure 8

Map shows the rainwater sampling site automatic weather station (AWS) at a high altitude in Shaune Garang catchment, Himachal Himalaya.

Supplementary Files

This is a list of supplementary files associated with this preprint. Click to download.

- SupplementaryInformation.docx